

# Documentation for $\frac{H}{E_L}P$ program, version 2

## *Theoretical manual & User guide*

Jan Vorel<sup>1</sup>

May 22, 2015

<sup>1</sup>Czech Technical University in Prague, Faculty of Civil Engineering, Department of Mechanics

# Contents

<b>1</b>	<b>Introduction</b>	<b>2</b>
1.1	Basic specifications and method . . . . .	2
<b>2</b>	<b>Theoretical manual</b>	<b>3</b>
2.1	Mori-Tanaka method . . . . .	3
2.1.1	Micro-scale . . . . .	3
2.1.2	Meso-scale . . . . .	5
<b>3</b>	<b>User guide</b>	<b>8</b>
3.1	Effective elastic properties and thermal conductivities . . . . .	8
3.2	Weave composite . . . . .	11
3.3	Input/Output file . . . . .	11

# Chapter 1

## Introduction

### 1.1 Basic specifications and method

Program **HE<sub>L</sub>P** (**H**eat and **E**lasticity **P**roperties) is a simple software for the determination of effective elastic properties and effective thermal conductivities using the Mori-Tanaka homogenization method. This program can be used for ellipsoidal inhomogeneities embedded in a generally anisotropic medium. **HE<sub>L</sub>P** was originally designed for evaluation of effective material properties of carbon-carbon plain weave textile composites on the micro- and meso-scale [11]. Therefore, the homogenization with the orientational averaging is also implemented.

# Chapter 2

## Theoretical manual

### 2.1 Mori-Tanaka method

In the last decade, effective media theories, widely used in classical continuum micro mechanics, have been recognized as an attractive alternative to FE based methods. Since its introduction the Mori-Tanaka (MT) method [8] has enjoyed a considerable interest in a variety of engineering applications. These include classical fiber matrix composites [1, 2], natural fiber systems [5], or even, although to a lesser extent, typical civil engineering materials such as asphalts [7] or cement pastes [12].

#### 2.1.1 Micro-scale

General description of the Mori-Tanaka method in the framework of elasticity and steady state heat conduction problem is outlined in this section. The notation introduced in [10] and [11] is employed.

The Mori-Tanaka method takes into account the effect of phase interactions on the local stresses by assuming an approximation in which the stress in each phase is equal to that of a single inclusion embedded into an unbounded matrix subjected to as yet unknown average matrix strain  $\boldsymbol{\varepsilon}_0 = \mathbf{A}_0 \mathbf{E}$ , where  $\mathbf{A}_0$  stands for the strain concentration factor and  $\mathbf{E}$  is the overall strain.

In Benvenistes reformulation of the Mori-Tanaka method [1], the local strain of a single inclusion in a large volume of matrix loaded by  $\boldsymbol{\varepsilon}_0$  assumes, for the local coordinate system  $x$  in Fig. 2.1, the form

$$\boldsymbol{\varepsilon}_r^x = \mathbf{T}_r^x \boldsymbol{\varepsilon}_0^x = \mathbf{A}_r^x \mathbf{E}^x, \quad (2.1)$$

where index 0 is reserved for the matrix and indexes 1, 2, ...,  $N$  for inclusions and  $\mathbf{T}_r$  is the partial strain concentration factor. The local strain on the phase can be decomposed into

$$\boldsymbol{\varepsilon}_r^x = \boldsymbol{\varepsilon}_0^x + (\mathbf{S} \boldsymbol{\varepsilon}_r^*)^x, \quad (2.2)$$

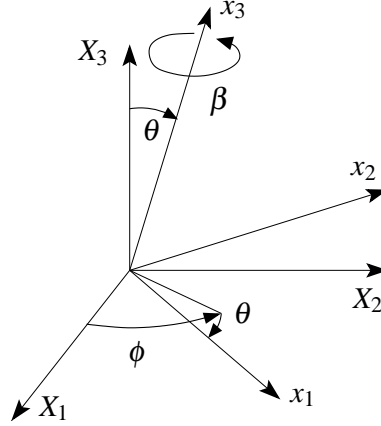


Figure 2.1: Local coordinate system and definition of the Euler angles.

where  $\boldsymbol{\varepsilon}_r^*$  represents a transformation strain in the homogenous, generally anisotropic, matrix to give the same local strain as in the composite. The tensor  $\mathbf{S}$  is known as the Eshelby tensor (see [9, 3] for more details). Combining Eq. (2.2) and  $\boldsymbol{\sigma}_r = \mathbf{L}_r \boldsymbol{\varepsilon}_r$  for the heterogeneity then gives

$$\boldsymbol{\sigma}_r^x = \mathbf{L}_r^x \boldsymbol{\varepsilon}_r^x = \mathbf{L}_0^x [\boldsymbol{\varepsilon}_r^x - (\boldsymbol{\varepsilon}_r^*)^x], \quad (2.3)$$

so that

$$(\boldsymbol{\varepsilon}_r^*)^x = (\mathbf{L}_0^x)^{-1} (\mathbf{L}_0^x - \mathbf{L}_r^x) \boldsymbol{\varepsilon}_r^x. \quad (2.4)$$

Next, substituting Eq. (2.4) into Eq. (2.2) provides

$$\boldsymbol{\varepsilon}_r^x = \boldsymbol{\varepsilon}_0^x + \mathbf{S}^x (\mathbf{L}_0^x)^{-1} (\mathbf{L}_0^x - \mathbf{L}_r^x) \boldsymbol{\varepsilon}_r^x, \quad (2.5)$$

and finally

$$\boldsymbol{\varepsilon}_r = [\mathbf{I} - \mathbf{S}^x (\mathbf{L}_0^x)^{-1} (\mathbf{L}_0^x - \mathbf{L}_r^x)]^{-1} \boldsymbol{\varepsilon}_0^x = \mathbf{T}_r^x \boldsymbol{\varepsilon}_0^x, \quad (2.6)$$

where  $\mathbf{I}$  is the identity matrix. In general, following [6], the overall average strain  $\mathbf{E}$  for a multi-phase composite with an orientation-dependent inclusion given in the global coordinate system  $\mathbf{X}$  then attains the form

$$\mathbf{E} = c_0 \boldsymbol{\varepsilon}_0 + \sum_{r=1}^N c_r \langle\langle \boldsymbol{\varepsilon}_r \rangle\rangle, \quad (2.7)$$

where  $c_r$  is the volume fraction of the phase  $r$  and the brackets  $\langle\langle \cdot \rangle\rangle$  denote averaging over all possible orientations. The global-local transformation is parametrized by three Euler angles  $(\phi, \theta, \beta)$ . Note that this transformation corresponds to successive rotation of global coordinate axes by angle  $\phi$  about the  $X_3$  axis, then by angle  $\theta$  about the new rotated  $x_2$  axis and finally to the rotation about the transformed  $x_3$  axis by angle  $\beta$  to obtain the local coordinate system.

Employing Eq.(2.1) the orientation average of  $\boldsymbol{\varepsilon}_r$  can be written as

$$\langle\langle \boldsymbol{\varepsilon}_r \rangle\rangle = \langle\langle \mathbf{T}_r \rangle\rangle \boldsymbol{\varepsilon}_0^x = \langle\langle \mathbf{A}_r \rangle\rangle \mathbf{E}^x. \quad (2.8)$$

Substitution of Eq. (2.1) into Eq. (2.7) and then into Eq. (2.8) leads to the relation for the concentration factor

$$\langle\langle \mathbf{A}_r \rangle\rangle = \langle\langle \mathbf{T}_r \rangle\rangle \left[ c_0 \mathbf{I} + \sum_{r=1}^N c_r \langle\langle \mathbf{T}_r \rangle\rangle \right]^{-1}. \quad (2.9)$$

With the help of the volume average of the overall stress

$$\Sigma = c_0 \sigma_0 + \sum_{r=1}^N c_r \langle\langle \sigma_r \rangle\rangle, \quad (2.10)$$

we obtain the effective stiffness matrix as

$$\mathbf{L} = \mathbf{L}_0 + \sum_{r=1}^N c_r [\langle\langle \mathbf{L}_r A_r \rangle\rangle - \mathbf{L}_0 \langle\langle A_r \rangle\rangle]. \quad (2.11)$$

### 2.1.2 Meso-scale

Plain weave textile composite (Fig. 2.2a,b) is a typical representative of composite system where the orientational averaging needs to be applied. If the idealized geometry of this material is assumed, the centerlines of the warp and fill systems of tows is described by a simple trigonometric form

$$c(x) = \frac{b}{2} \sin\left(\frac{\pi x}{a}\right). \quad (2.12)$$

It is assumed that all fibres within the tow are oriented parallel to the centreline. The exact joint probability function describing the distribution of individual Euler angles for the warp tow has the form presented in [10]. In this program, however, an approximation of this function in the form, see also Fig. 2.2c,d,

$$g(\theta, \phi, \beta) = \begin{cases} 1/(2\alpha) & \text{if } \theta = 0, \beta = 0 \text{ and } -\alpha \leq \theta \leq \alpha, \\ 0 & \text{otherwise,} \end{cases} \quad (2.13)$$

where

$$\alpha = \arctan\left(\frac{b\pi}{2a}\right), \quad (2.14)$$

is used. Following [10] where the composite is viewed as a two-phase composite, the resulting homogenized stiffness matrix given by Eq. (2.11) becomes

$$\mathbf{L} = \mathbf{L}_0 + \frac{c_1}{2} [\langle\langle \mathbf{D}^{\text{warp}} \rangle\rangle + \langle\langle \mathbf{D}^{\text{fill}} \rangle\rangle], \quad (2.15)$$

where  $\mathbf{D}$  represents an orientation dependent quantity

$$\langle\langle \mathbf{D} \rangle\rangle = \langle\langle \mathbf{L}_1 \mathbf{A}_1 \rangle\rangle - \mathbf{L}_0 \langle\langle \mathbf{A}_1 \rangle\rangle, \quad (2.16)$$

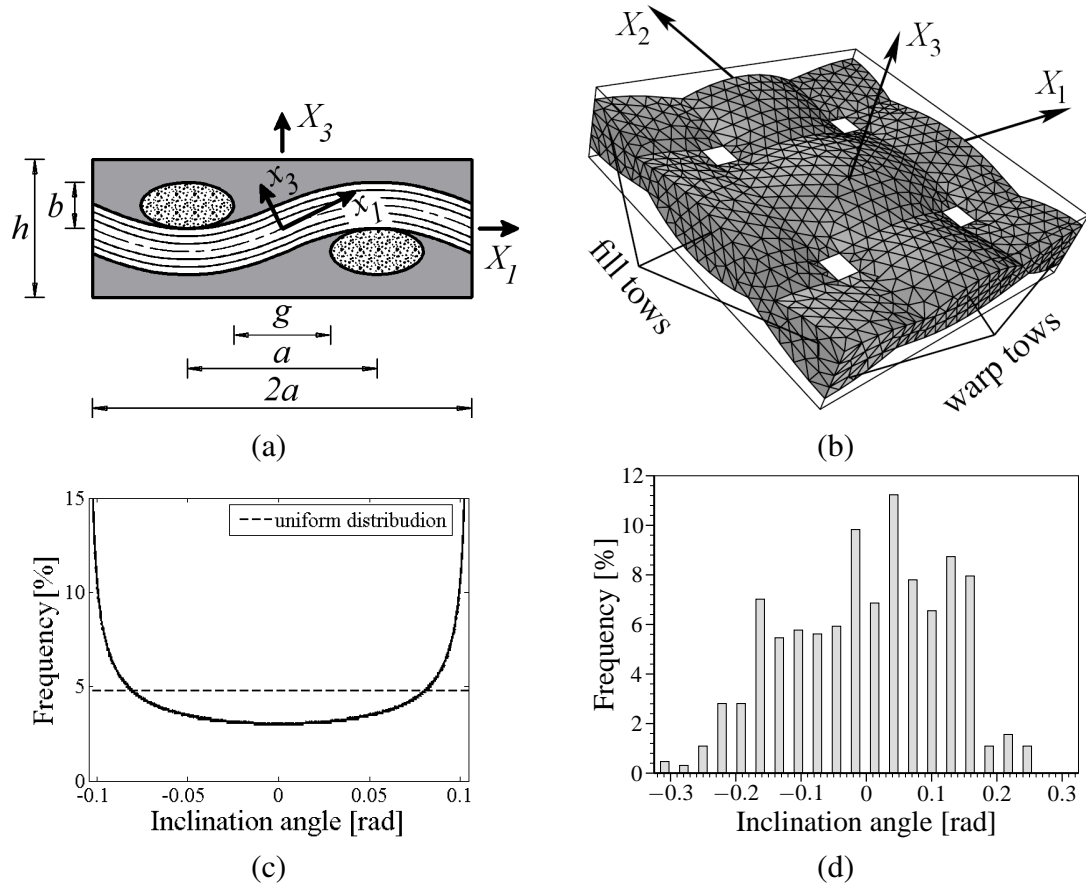


Figure 2.2: Ideal periodic unit cell: (a) cross-section, (b) three-dimensional view, (c) approximate distribution of inclination angles, (d) example of a real distribution of inclination angles

where

$$\mathbf{A}_1 = \mathbf{T}_1 (c_0 \mathbf{I} + c_1 \mathbf{T}_1)^{-1}. \quad (2.17)$$

For the warp system  $\langle\langle \mathbf{D} \rangle\rangle$  is written as

$$\langle\langle \mathbf{D}^{\text{warp}} \rangle\rangle = \int_{-\alpha}^{\alpha} g(\phi, \theta, \beta) \mathbf{D}(0, \theta, 0) d\theta, \quad (2.18)$$

and similarly for the fill system we get

$$\langle\langle \mathbf{D}^{\text{fill}} \rangle\rangle = \int_{-\alpha}^{\alpha} g(\phi, \theta, \beta) \mathbf{D}\left(\frac{\pi}{2}, \theta, 0\right) d\theta. \quad (2.19)$$

If the composite is taken as a three-phase composite, the effective stiffness matrix attains a slightly different form

$$\mathbf{L} = \mathbf{L}_0 + \frac{c_1}{2} \left[ \langle\langle \mathbf{L}^{\text{warp}} \mathbf{A}^{\text{warp}} + \mathbf{L}^{\text{fill}} \mathbf{A}^{\text{fill}} \rangle\rangle - \mathbf{L}_1 \langle\langle \mathbf{A}^{\text{warp}} + \mathbf{A}^{\text{fill}} \rangle\rangle \right], \quad (2.20)$$

where

$$\mathbf{A}^{\text{warp}} = \mathbf{T}^{\text{warp}} \left[ c_0 \mathbf{I} + \frac{c_1}{2} (\mathbf{T}^{\text{warp}} + \mathbf{T}^{\text{fill}}) \right]^{-1}, \quad \mathbf{T}^{\text{warp}} = \mathbf{T}^{\text{warp}}(0, \theta, 0), \quad (2.21)$$

$$\mathbf{A}^{\text{fill}} = \mathbf{T}^{\text{fill}} \left[ c_0 \mathbf{I} + \frac{c_1}{2} (\mathbf{T}^{\text{warp}} + \mathbf{T}^{\text{fill}}) \right]^{-1}, \quad \mathbf{T}^{\text{fill}} = \mathbf{T}^{\text{fill}}\left(\frac{\pi}{2}, \theta, 0\right). \quad (2.22)$$

The evaluation of the homogenized thermal conductivity matrix proceeds similarly. The second order tensor  $\mathbf{S}$  for the conduction problem analogous to the Eshelby tensor can be derived through the relations presented in [4, 6].



# Chapter 3

## User guide

Program  $HE_{LP}$  offers a user friendly environment. It allows us to address three major topics:

- Evaluation of the effective elastic properties of multi-phase composites with aligned inclusions of the ellipsoidal shape
- Evaluation of the effective thermal conductivities of multi-phase composites with aligned inclusions of the ellipsoidal shape
- Evaluation of the effective elastic properties and effective thermal conductivities of textile composites

All sheets are designed in a similar way. The program window has common tool strip buttons on the top of the window and is divided into four parts, (Fig. 3.1)

### 3.1 Effective elastic properties and thermal conductivities

These program sheets serve to determine the effective (homogenized) stiffness and conductivity matrices, respectively. As shown in Fig. 3.1, the top part of the main window (group box “*Matrix*”) is reserved for the material parameters of the matrix phase where as the material parameters of the inclusion (group box “*Inclusion*”) are assigned in the middle part of the main window. The results (group box “*Results*”) are displayed at the bottom of the main window.

The number of required parameters to input depends on the degree of material anisotropy of a given phase. The inclusion section is designed as to add or remove an arbitrary number of inclusions. Apart from the material parameters this section requires specifying shape of the inclusion, Euler angles and volume fraction, see Fig. 3.2 for the example of the evaluation of effective thermal conductivities.

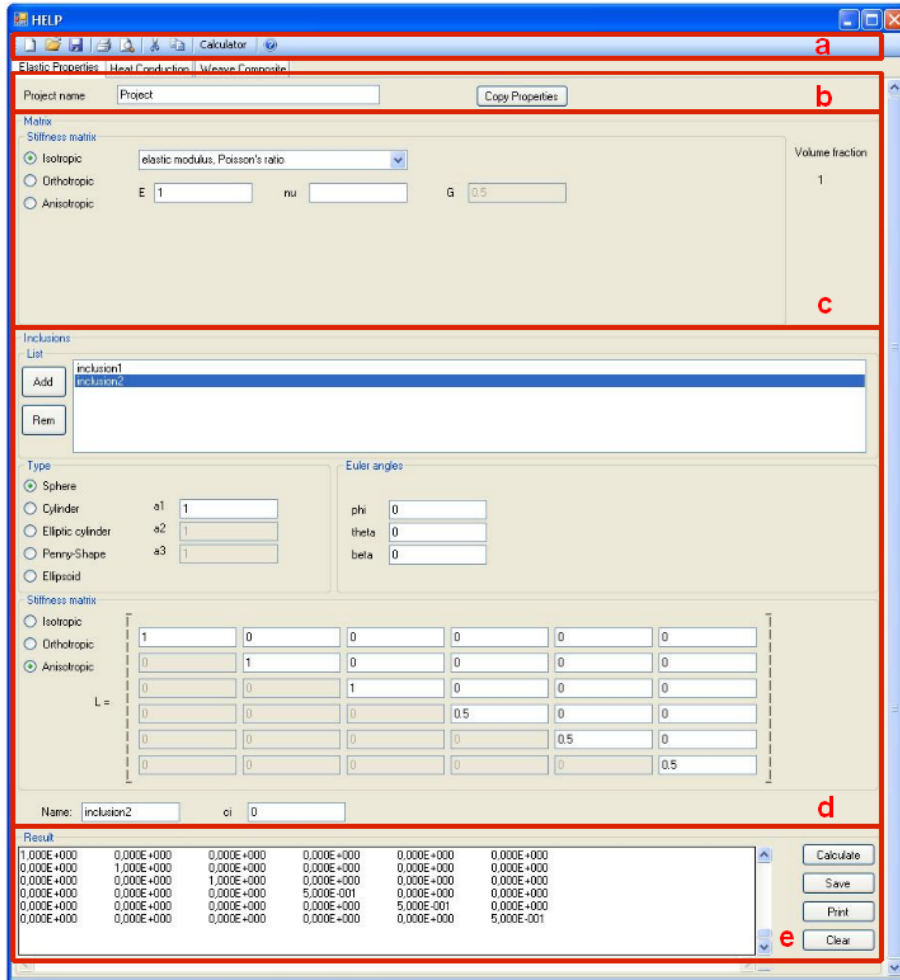


Figure 3.1: HE<sub>L</sub>P window structure: a) common tool strip buttons, b) general informations, c) matrix properties, d) inclusions (tows) properties, e) result viewer

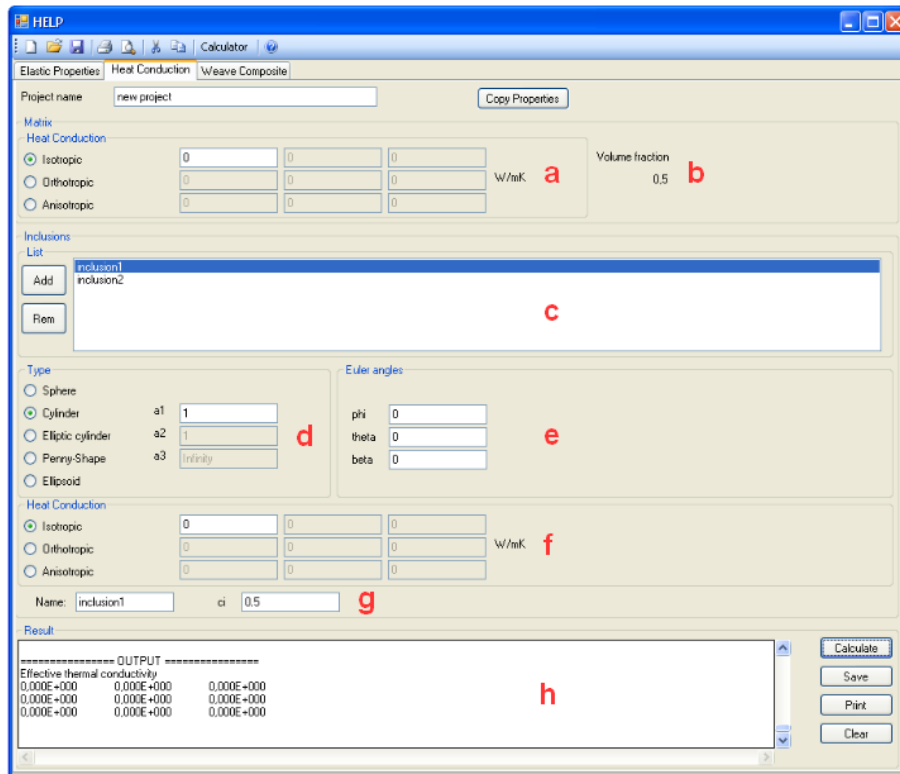


Figure 3.2: Heat conduction: a) thermal conduction matrix, b) matrix volume fraction, c) inclusion list, d) semi-axes, e) Euler angles, f) material properties for an inclusion, g) name and volume fraction, h) output window

## 3.2 Weave composite

There are only minor changes in the input when compared to more simple composite aggregates discussed in the previous section. First, the problem (elasticity or thermal conduction) must be selected (Fig. 3.3a). Then the dimensions of the periodic unit cell (PUC) are required (Fig. 3.3b). The quantities signs are the same as in Fig. 2.2a. The matrix material properties are assigned in the same way as above. The “*Tow*” box serves to specify the effective properties of perpendicular bundles. The common volume fraction for the fill and warp system of tows is assumed, see Fig. 3.3d. The shape of the bundle is define through its semi-axes (Fig. 3.3e) and orientation with respect to the global coordinate system using again the Euler angles (Fig. 3.3f). The required material parameters are introduced next again depending on the selected type of the material symmetry in the bundle local coordinate system. Note that the local  $x_1$  axis is aligned with the fiber direction. As discussed in the theoretical part of this manual, it is also required to chose the type of analysis (Fig. 3.3h), recall Eqs. (2.15,2.20).

## 3.3 Input/Output file

The input/output project files including the matrix and inclusions (tows) parameters are stored in the “XML” format and are assigned the file name extension “.XMLH”. Note that only the active sheets are saved when pressing the save bottom on the top tool strip of the main window. The same applies when loading the project. The structure of these files can be seen by generating an output file from the **HEL**P program.

There are two possibilities to save the results displayed in the output window when pressing the save bottom on the right bottom part of the main window. The first is to save the whole text in the specified text file. The other option is based on standard copy and paste operations.

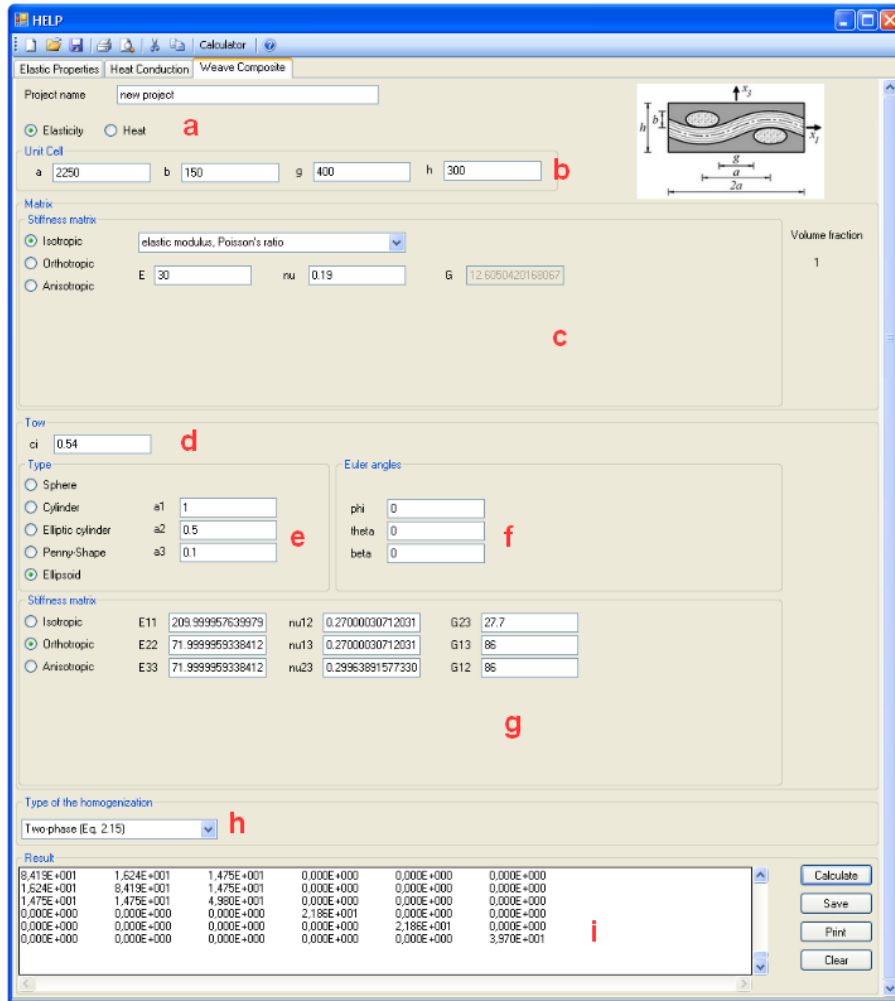


Figure 3.3: Weave composite: a) problem type, b) PUC dimensions, c) matrix properties, d) tows volume fraction, e) semi-axes, f) Euler angles, g) material properties for bundles, h) homogenization type, i) output window

# List of Figures

2.1	Local coordinate system and definition of the Euler angles. . . . .	4
2.2	Ideal periodic unit cell: (a) cross-section, (b) three-dimensional view, (c) approximate distribution of inclination angles, (d) example of a real distribution of inclination angles . . . . .	6
3.1	<b>HE<sub>L</sub>P</b> window structure: a) common tool strip buttons, b) general informations, c) matrix properties, d) inclusions (tows) properties, e) result viewer . . .	9
3.2	Heat conduction: a) thermal conduction matrix, b) matrix volume fraction, c) inclusion list, d) semi-axes, e) Euler angles, f) material properties for an inclusion, g) name and volume fraction, h) output window . . . . .	10
3.3	Weave composite: a) problem type, b) PUC dimensions, c) matrix properties, d) tows volume fraction, e) semi-axes, f) Euler angles, g) material properties for bundles, h) homogenization type, i) output window . . . . .	12

# Bibliography

- [1] Y. Benveniste, *A new approach to the application of Mori-Tanaka theory in composite materials*, Mechanics of Materials **6** (1987), 147–157.
- [2] G.J. Dvorak and M. Sejnoha, *Initial failure maps for ceramic and metal matrix composites*, Modelling Simul. Mater. Sci. Eng. **4** (1996), 553–580.
- [3] A.C. Gavazzi and D.C. Lagoudas, *On the numerical evaluation of eshelby's tensor and its application to elastoplastic fibrous composites*, Computational Mechanics **7** (1990), 13–19.
- [4] H. Hatta and M. Taya, *Equivalent inclusion method for steady state heat conduction in composites*, International Journal of Engineering Science **24** (1986), 1159–1170.
- [5] Ch. Hellmich and F.-J. Ulm, *Drained and undrained poroelastic properties of healthy and pathological bone: a poro-micromechanical investigation*, Transp Porous Med **58** (2005), 243–268.
- [6] H. Jeong, D.K. Hsu, and P.K. Liaw, *Anisotropic conductivities of multiphase particulate metal-matrix composites*, Composite Science and Technology **58** (1998), 65–76.
- [7] R. Lackner, M. Spiegl, R. Blab, and J. Eberhardsteiner, *Is low-temperature creep of asphalt mastic independent of filler shape and mineralogy? - arguments from multiscale analysis*, Journal of Materials in Civil Engineering, ASCE **15** (2005), 485–491.
- [8] T. Mori and K. Tanaka, *Average stress in matrix and average elastic energy of elastic materials with misfitting inclusions*, Acta Metallurgica **21** (1973), 571.
- [9] T. Mura, *Micromechanics of defects in solids*, second revised ed., Mechanics of elastic and inelastic solids, no. 3, Kluwer Academic Publishers, 1987.
- [10] J. Škoček, J. Zeman, and M. Šejnoha, *Effective properties of Carbon-Carbon textile composites: application of the Mori-Tanaka method*, Modelling and Simulation in Materials Science and Engineering **0** (2008), 0–0, Accepted.

- [11] J. Vorel and M. Šejnoha, *Evaluation of homogenized thermal conductivities of imperfect carbon-carbon textile composites using the mori-tanaka method*, Structural Engineering and Mechanics (2008), Submitted.
- [12] V. Šmilauer and Z. Bittnar, *Microstructure-based micromechanical prediction of elastic properties in hydrating cement paste*, Cement and Concrete Research **36** (2006), no. 9, 1708–1718.